

Overlap Friction Stir Welding and Adhesive Bonding AA6082 joints Fatigue

Ricardo Maciel¹, Tiago Bento¹, Daniel F. O. Braga¹, Lucas da Silva², Pedro Moreira³, and Virginia Infante⁴

¹IDMEC

²Universidade do Porto Faculdade de Engenharia

³INEGI

⁴Affiliation not available

May 5, 2020

Abstract

Even though friction stir welding (FSW) has been shown to produce high performing butt-joints, stress concentration at the weld edges in overlap FSW significantly reduces the performance of these joints. By combining FSW and adhesive bonding into a friction stir (FS) weld-bonding, joint mechanical performance is greatly improved. Quasi-static and fatigue strength of the proposed FS weld-bonding joints was assessed and benchmarked against overlap FSW and adhesive bonding. The characterization of the structural adhesive is also presented, including differential scanning calorimetry (DSC) and thermogravimetric analysis (TGA), as well as mechanical characterization with curing temperature. A small process parameter study was made to select proper FSW parameters for AA6082-T6 overlap FSW and FS weld-bonded joints. The adhesive degradation temperature (357°C) was found to be higher than reported temperatures in the adhesive during welding of FS weld-bonding joints. Higher curing temperatures were found to lead to increased strength while decreasing ductility of the adhesive. The addition of adhesive bonding to the overlap FSW to produce FS weld-bonding resulted in a significant increase in quasi-static and fatigue strength, achieving 79.9% of the fatigue strength of adhesive bonded joints at 106 cycles, while FSW had 41.6%.

Introduction

Various drivers have pushed for the development and implementation of new joining processes in lightweight metal structures. One technology that has shown significant potential is FSW given the solid-state nature of the joining process. However, when welding large shell structures such as aeronautical fuselage panels, gaps may arise between the abutting faces to join leading to significant degradation of the joint mechanical properties when butt-welding.¹ Overlap FSW can overcome this limitation, but the edge of the weld in the advancing side forms a hook like defect, which diminishes the joint strength.^{2,3} To improve strength in this joint configuration it has been proposed to use multiple pass welding.³ By employing this method, the out of plane bending and peel load at these unwelded tips is reduced. This method, however, comes with disadvantages of its own. To accommodate the shoulder diameter and clamping, the overlaps must be larger, diminishing the weight savings gains. Lead time is also increased, along with tool wear, making the process less economically viable. Another way of improving the strength of overlap FSW joints is by combining it with another joining method such as adhesive bonding, resulting in FS weld-bonding. This way the adhesive layer at the edges increases effective overlap and reduces peel stress at the weld edges. This method was used in magnesium-to-aluminum friction stir spot welded joints, resulting in increased quasi-static and fatigue

strength.⁴ Similarly this method was proposed for continuous joints of AA2024-T3, resulting in improved quasi-static and fatigue strength.⁵

This study covers hybrid overlap FSW and adhesive bonding of an Al-Mg alloy (AA6082-T6), which is a common multi-purpose alloy. Characterization of the adhesive used in the study is first presented, including the effect of curing temperature in mechanical performance. This is relevant given that the adhesive in FS weld-bonded joints will not cure all at the same temperature. The degradation temperature is also measured through thermogravimetric analysis, to assess if it is below temperatures achieved during welding. FSW process parameters for FSW and FS weld-bonded joints were then studied to find a set that results in sound quality joints. Finally, the joints were subjected to cyclic loading at $R=0.1$ to assess the fatigue performance.

Experimental Details

When joining large components as in the case of longitudinal fuselage joints, it may not be feasible to control curing temperature evenly and as such, an adhesive capable of both curing at room temperature and elevated temperature is desirable. During FSW of FS weld-bonded joints, the uncured adhesive will be subjected to an elevated temperature which may locally accelerate the curing process. To assess the curing process of the chosen adhesive differential scanning calorimetry (DSC) was used. DSC analysis was performed on a Netzsch[®] DSC 200 F3 equipment on specimens with a mass of [?]50 mg, at a constant heating rate of 20 K/min from 21oC to 320oC in an atmosphere of constant flow of 20 mL/min of N₂. Figure 1 shows a representative curve of a DSC analysis.

Figure 1 Representative curve of DSC analysis of the uncured epoxy adhesive

Even though the adhesive may cure at room temperature, DSC analysis showed that the majority of the curing process occurs at elevated temperatures, with peak curing at [?]120oC. An endothermic event is also observed at about 200oC in all samples tested, which is believed to be evaporation of water, after exceeding the sealing limit of the sample container (water vapor pressure at 200oC is [?]15 Atm).

From the DSC analysis it may be inferred that full curing does not occur at room temperature, leading the adhesive to have different mechanical behavior with different curing conditions. To assess the tensile mechanical properties of the adhesive, bulk tensile were performed at 1 mm/min crosshead speed in an Instron testing machine. The bulk tensile specimens were made with 4 different curing conditions, room temperature for 7 days, 120oC for 1 hour as indicated in the adhesive data sheet, 165oC and 200oC for 30 minutes. After curing specimens were milled according to ASTM D638 standard. In Figure 2, the resulting stress vs strain curves for the 4 curing conditions are presented.

Figure 2 Representative Araldite 420 stress vs. strain curves with curing temperature

An increase in ultimate strength was observed with increasing curing temperature, accompanied by a reduction in elongation at break. This behavior may be due to increased cross-linking of the polymeric chains with increasing cure temperature. The change is more significantly from room temperature to 120oC cure condition than from 120oC to further higher temperatures. This is consistent with the DSC analysis results where most of the curing was shown to happen around 120oC.

As during the welding process, the adhesive will be subjected to high temperatures, having an adhesive with a high degradation temperature is important. Thermogravimetric analysis (TGA) of the uncured epoxy adhesive was made on a Netzsch(r) Tg209 F3 Tarsus at 20 K/min from 21oC to 600oC. Figure 3 presents resulting TG curves where the onset of degradation was found to be at 357_{-3}^{+2} oC. Temperatures in the adhesive during FS weld-bonding were reported to be between 200oC and 250oC, which leads to conclude that no significant degradation will occur during the welding procedure.⁶

Figure 3 TGA of uncured epoxy adhesive

To determine shear strength and shear modulus, thick adherend shear test (TAST) and Poisson ratio measurement were made according to ASTM D5656 – 10 and ASTM E132 – 17 respectively. Two curing conditions were assessed, room temperature for 1 week and 120oC for 1 hour. The resulting (τ_u) and shear modulus are presented in Table 1.

Given the complex loading case of single lap joints, with combination of peel and shear load on the adhesive, fracture toughness of the adhesive in mode I and II was assessed through double cantilever beam (DCB) specimens and end notch flexure (ENF) specimens. In both tests, specimens had the same dimensions, being composed of two steel beams with 320 x 25 x 12.7 mm bonded by a layer of 0.2 mm thick adhesive, differing only on the loading method. Specimens used for fracture toughness assessment were cured at room temperature for 7 days and as an approximation it was assumed that fracture toughness remained unchanged with curing condition. However, it may be expected that some fracture toughness is lost with increasing curing temperature and as such the real values may be lower.⁷

DCB specimens were loaded at 1 mm/min crosshead speed and the resulting load vs. displacement curves were used to plot the corresponding R-curves using the compliance based beam method (CBBM).⁸ A resulting representative R-curve is shown in Figure 4. The critical fracture toughness in mode I measured was 3 ± 0.37 N/mm. This value is relatively high compared with other structural adhesives^{9,10} and continuous fiber reinforced composites¹¹, showing that the chosen epoxy has high fracture resistance.

Figure 4 Representative adhesive R-curve for mode I

A digital twin of the experimental procedure was created to confirm measured experimental data using Abaqus. Cohesive zone modeling (CZM) was used to model the adhesive failure. The load vs. displacement curves were in good agreement as shown in Figure 5.

Figure 5 a) von Mises stress in 3D DCB Abaqus model at 5 mm displacement and b) load displacement curve comparison between numeric and experimental

For mode II, ENF testing was performed at 0.2 mm/min crosshead speed. Similarly to the DCB tests in mode I, the ENF tests were also analyzed through CBBM method, but in this case for mode II loading.¹² A representative R-curve obtained in the ENF tests is presented in Figure 6. The critical fracture toughness measured in mode II was 11.6 ± 0.3 N/mm. However, the maximum bending load was relatively high, which may have induced local plasticization, and as such the measured mode II fracture toughness may be artificially high. A parametric study was then used to find an adequate adhesive fracture toughness in mode II, by keeping constant all other material parameters and comparing numeric and experimental loads vs displacement curves.

Figure 6 Representative adhesive R-curve for mode II

The Abaqus model showed that indeed 11.6 N/mm was an overestimation of the critical fracture toughness in mode II and by an iterative process that 9 N/mm resulted in better agreement with the experimental load vs. displacement curves as shown in Figure 7. This value is still relatively high fracture strength when compared with adhesives reported in the literature.^{13,14} There was a small difference in terms of stiffness between numerical model and experimental data which was consistent in all numeric runs and is probably due to the experimental loading configuration. As the ENF test is performed in 3-point bending, the machine is operated in compression and the displacement values measured include all the slack within the system, while in the numerical model no such limitations exist.

Figure 7 a) Shear stress in 3D ENF Abaqus model at the onset of damage, b) displacement curve comparison between numeric and experimental.

The adhesive mechanical properties are summarized in Table 1, for two curing conditions.

Table 1 - Araldite 420 mechanical properties

The alloy used in this study was the AA6082-T6. The chemical composition is shown in Table 2 and the mechanical properties in Table 3.

Table 2 Chemical composition of AA6082-T6(% mass)¹⁵

Table 3 AA6082-T6 mechanical properties¹⁵

All welding procedures were performed on a dedicated FSW ESAB^(x) LEGIO 3UL numerical control machine. In FS weld-bonding, the welding procedure was done with the adhesive in a non-cured state and right after adhesive lay-up and joint closing. Calibrated metal strips with 0.2 mm thickness were strategically positioned in-between the shim plates to assure a more uniform adhesive thickness.

Prior to bonding surfaces to be bonded were degreased and sanded. In the case of adhesive bonded joints phosphoric acid anodization (PAA) according to ASTM D3933 - 98(2017) standard was used, while FS weld-bonded joints were subjected to chemical treatment with 3M^(x) AC-130, which is a sol-gel anodization replacement normally intended for aeronautical repair¹⁶.

The FSW tool used had 5 mm diameter cylindrical threaded pin with 3 mm length and 16 mm diameter grooved shoulder. The FSW process parameters used are listed in Table 4. These were chosen based on literature review and past experience. Various levels of downward force were tested to assess its effect on joint performance and maximize joint strength.

Table 4 FSW process parameters

All joint configurations were tensile tested with three specimens each. Tensile testing was done in an Instron^(x) 5566 machine at 1 mm/min crosshead speed. Joint efficiency was calculated dividing maximum axial load by the substrate cross-section outside of the overlap as in previous works.^{3,17} Figure 8, compares the joint efficiency of the joint configurations tested.

Figure 8 Joint efficiency of FSW and FS weld-bonded joints with differing downward force

When comparing FS weld-bonded joints to FSW it was possible to observe an improvement of 20-30 % in most cases. It was possible to observe that for FSW joints the increase in downward force results in an increase of joint strength. This may be related with higher thermal input which leads to further softening of the workpiece. The further softening of the workpiece may result in better mixing and as such diminishing the hook defect size, as presented in.¹⁸ For FS weld-bonded joints the trend is not as clear as in FSW joints, as it increases from 400 to 450 kgf but diminishes from then on. The reasoning for this decrease may be due to high downward force leading to excessive adhesive thinning or possibly the higher temperature may lead to degradation of the surface to bond and/or the adhesive. FS weld-bonded joints also showed higher dispersion in terms of joint strength than FSW which may be due to variations in surface treatment, as the joint strength is very sensitive to the bonding strength. Figure 9, compares the highest strength FSW and FS weld-bonded joints with adhesive bonded joints.

Figure 9 Stress vs. displacement of highest strength FSW and FS weld-bonded joints along the adhesive bonded.

In Figure 10, the microhardness profile and joint cross-section of the best performing FS weld-bonded joint is presented. It is possible to observe that the hook defect formed by the upward flow of material generated in the advancing side is present. The size and shape of this defect is critical to overlap FSW joint strength.¹⁸ Along with the hook defect it is also observable a cold lap defect on the retreating side of the weld, which is a result of the initial upward flow under shearing effect of the pin followed by a downward flow in order to fill the space at the bottom of the pin. However, these defects become less critical in FS weld-bonded joints when compared to FSW as the adhesive increases the effective joined overlap and reduces loading the weld edges.

Figure 10 a) Microhardness profile and b) joint cross-section of FS weld-bonded joint with 450 kgf

A loss of hardness is presented in the microhardness profile, which is due to the loss of T6 condition during welding. Temperatures increase towards the top of the joint due to contact between workpiece and tool and as such, a wider cross-section of the joint has lower hardness at the top.

An assessment of the fatigue strength of FSW, FS weld-bonded and adhesive bonded joints was then made at a load ratio of $R=0.1$ in an Instron 8874 machine. For this study both FSW and FS weld-bonded joints were made using 450 kgf. Figure 11 shows the resulting S-N curves including 50% and 5% probability of failure calculated using ProFatigue software.¹⁹ The S-N curve regarding the AA6082-T6 base material reported in²⁰ was also included.

Figure 11 a) p-S-N curves of the three joint type and b) failure modes

FSW joints showed lower fatigue strength than adhesive and FS weld-bonded joints as it would be expected given the lower quasi-static strength. The FS weld-bonded showed similar fatigue strength to adhesive bonded joints. Adhesive bonded joints still had the highest fatigue strength of all joints tested, which is to be expected given the more continuous stress distribution in these joints. At 10^6 cycles adhesive bonded joints have a 50% probability of failure at 56.4 MPa, while FS weld-bonding and FSW at the same number of cycles the 50% probability of failure is achieved at 45.1 MPa (79.9% of adhesive bonded joints) and 23.5 MPa (41.6% of adhesive bonded joints). The failure modes were consistent with the quasi-static ones, with the adhesive failing in adhesive/cohesive way, the FSW failing through the hook defect and the FS weld-bonded ones failing through the adhesive layer followed by cracking through the hook.

Concluding Remarks

The combination of FSW and adhesive bonding into friction stir weld-bonding was studied regarding quasi-static and fatigue performance. In order to benchmark the process, it was compared against overlap FSW and adhesive bonding.

The epoxy adhesive used was characterized taking into consideration the curing temperature, showing that even though it cures at room temperature, higher temperature curing will increase strength while reducing ductility. Degradation temperature was also found to be above reported temperatures incurred during the welding procedure.

In the joints quasi-static testing, overlap FSW showed lower strength and ductility than FS weld-bonding joints. Downward force during welding, showed a significant effect in strength and ductility of FSW joints, with both increasing up to 550 kgf. The same trend was not observed in the FS weld-bonded joints, with the highest strength and ductility achieved at 450 kgf, with a joint efficiency of 94.96%. In FS weld-bonded joints the critical weld edges were kept close by the adhesive, leading to increase mechanical performance. As such, adhesive strength and the quality of the surface treatment are more significant to joint strength than downward force during welding. Adhesive bonded joints showed the highest strength and ductility given the relatively large overlap.

In cyclic loading at $R=0.1$, similar trends to the quasi-static loading were observed. Adhesive bonding achieved the highest fatigue strength followed by FS weld-bonding and FSW showed significantly lower fatigue strength (41.6% strength of adhesive bonded joints at 10^6 cycles). The hook defect serves as a fatigue crack initiation location and leads to the failure of FSW joints. Adhesive joints fail in an adhesive / cohesive manner, while FS weld-bonding fail through the adhesive immediately followed by cracking through the hook defect.

Acknowledgements

This work was supported by FCT, through IDMEC, under LAETA, project UIDB/50022/2020. Funding provided from NORTE-01-0145-FEDER-000022 SciTech – Science and Technology for Competitive and

Sustainable Industries is acknowledged. The authors acknowledge the funding provided by FCT project PTDC/EME-EME/29340/2017 – DisFri.

References

1. Shultz EF, Cole EG, Smith CB, Zinn MR, Ferrier NJ, Pfefferkorn FE. Effect of Compliance and Travel Angle on Friction Stir Welding With Gaps. *Journal of Manufacturing Science and Engineering*.2010;132(4).
2. Fersini D, Pironi A. Fatigue behaviour of Al2024-T3 friction stir welded lap joints. *Engineering Fracture Mechanics*.2007;74(4):468-480.
3. Papadopoulos M, Tavares S, Pacchione M, Pantelakis S. Mechanical behaviour of AA 2024 friction stir overlap welds. *International Journal of Structural Integrity*. 2013;4(1):108-120.
4. Chowdhury SH, Chen DL, Bhole SD, Cao X, Wanjara P. Lap shear strength and fatigue behavior of friction stir spot welded dissimilar magnesium-to-aluminum joints with adhesive. *Materials Science and Engineering: A*. 2013;562:53-60.
5. Braga DFO, Maciel R, Bergmann L, et al. Fatigue performance of hybrid overlap friction stir welding and adhesive bonding of an Al-Mg-Cu alloy. *Fatigue & Fracture of Engineering Materials & Structures*.2019;42(6):1262-1270.
6. Braga DFO. *Innovative structural joining for lightweight design* [PhD], Faculty of Engineering of the University of Porto; 2018.
7. Incerti D, Wang T, Carolan D, Fergusson A. Curing rate effects on the toughness of epoxy polymers. *Polymer*. 2018;159:116-123.
8. de Moura MFSF, Dourado N. Mode I fracture characterization of wood using the TDCB test. *Theoretical and Applied Fracture Mechanics*.2018;94:40-45.
9. Banea MD, Silva LFMd, Campilho RDSG. Effect of Temperature on Tensile Strength and Mode I Fracture Toughness of a High Temperature Epoxy Adhesive. *Journal of Adhesion Science and Technology*.2012;26(7):939-953.
10. de Moura MFSF, Campilho RDSG, Goncalves JPM. Crack equivalent concept applied to the fracture characterization of bonded joints under pure mode I loading. *Composites Science and Technology*.2008;68(10):2224-2230.
11. Machado JJM, Marques EAS, Campilho R, da Silva LFM. Mode I fracture toughness of CFRP as a function of temperature and strain rate. *Journal of Composite Materials*. 2016;51(23):3315-3326.
12. de Moura MFSF, Silva MAL, de Moraes AB, Moraes JJJ. Equivalent crack based mode II fracture characterization of wood. *Engineering Fracture Mechanics*. 2006;73(8):978-993.
13. de Moura MFSF, Campilho RDSG, Goncalves JPM. Pure mode II fracture characterization of composite bonded joints. *International Journal of Solids and Structures*. 2009;46(6):1589-1595.
14. Azevedo JCS, Campilho RDSG, da Silva FJG, Faneco TMS, Lopes RM. Cohesive law estimation of adhesive joints in mode II condition. *Theoretical and Applied Fracture Mechanics*. 2015;80:143-154.
15. Matweb. <http://www.matweb.com>, 2020.
16. McCray D, Smith J, Mazza J, Storage K. *Evaluation of adhesive bond primers for repair bonding of aluminum*. AIR FORCE RESEARCH LAB WRIGHT-PATTERSON AFB OH MATERIALS AND MANUFACTURING ...;2011.
17. Infante V, Braga DFO, Duarte F, Moreira PMG, de Freitas M, de Castro PMST. Study of the fatigue behaviour of dissimilar aluminium joints produced by friction stir welding. *International Journal of Fatigue*. 2016;82:310-316.

18. Maciel RL, Infante V, Braga D, Moreira P, Bento T, da Silva L. Development of hybrid friction stir welding and adhesive bonding single lap joints in aluminium alloys. *Frattura ed Integrità Strutturale*. 2019;13(48):269-285.

19. Fernandez-Canteli A, Przybilla C, Nogal M, Aenlle ML, Castillo E. ProFatigue: A Software Program for Probabilistic Assessment of Experimental Fatigue Data Sets. *Procedia Engineering*. 2014;74:236-241.

20. Moreira PMGP, Richter-Trummer V, de Castro PMST. Fatigue Behaviour of FS, LB and MIG Welds of AA6061-T6 and AA6082-T6. Paper presented at: Multiscale Fatigue Crack Initiation and Propagation of Engineering Materials: Structural Integrity and Microstructural Worthiness; 2008//, 2008; Dordrecht.

Hosted file

Table 1.docx available at <https://authorea.com/users/297375/articles/426489-overlap-friction-stir-welding-and-adhesive-bonding-aa6082-joints-fatigue>

Hosted file

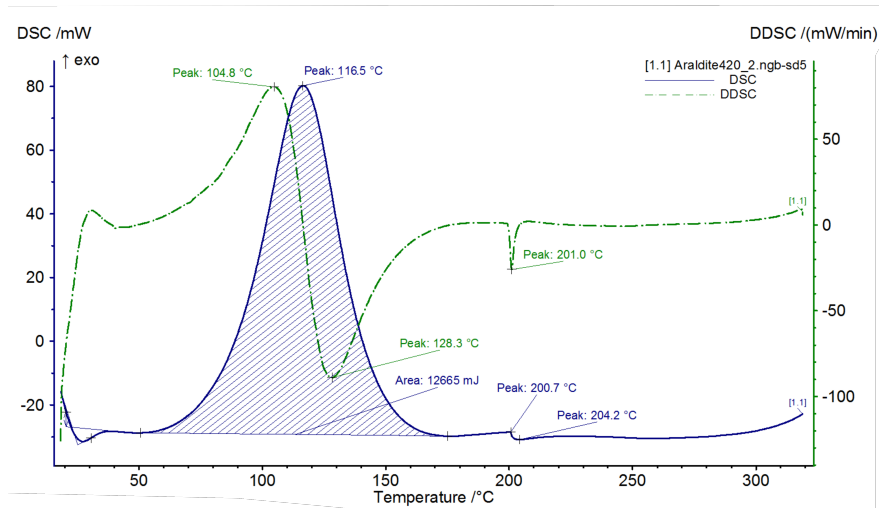
Table 2.docx available at <https://authorea.com/users/297375/articles/426489-overlap-friction-stir-welding-and-adhesive-bonding-aa6082-joints-fatigue>

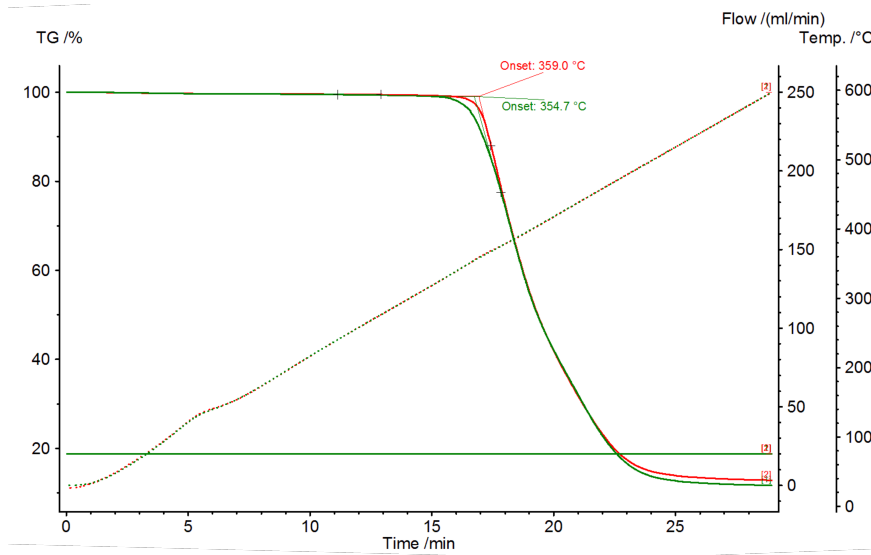
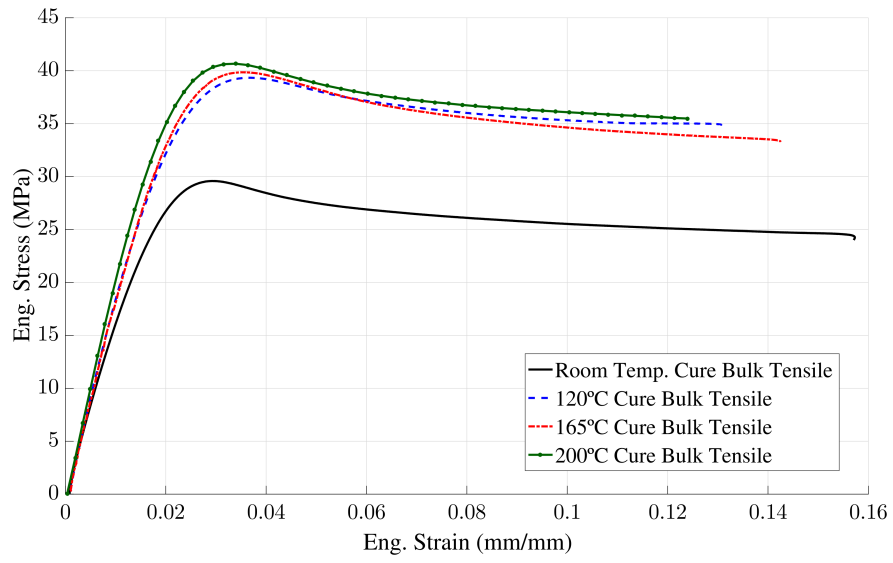
Hosted file

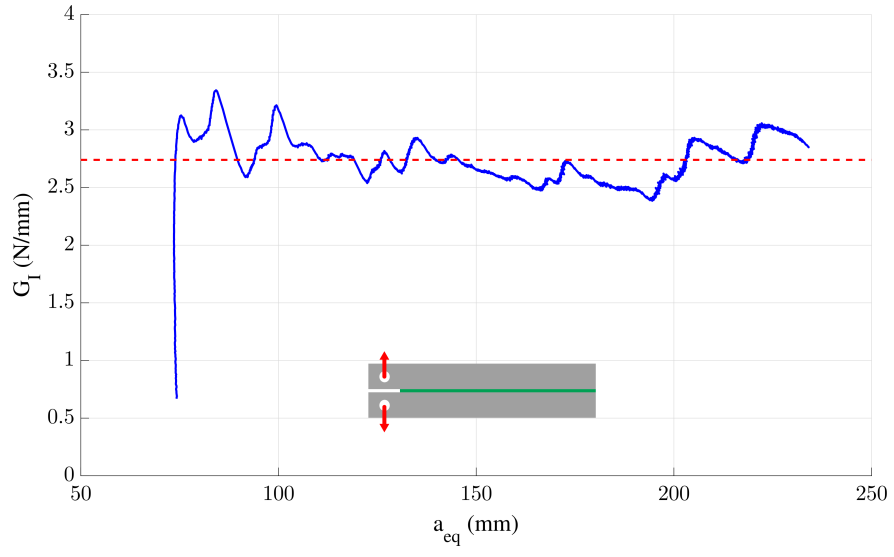
Table_3 (1).docx available at <https://authorea.com/users/297375/articles/426489-overlap-friction-stir-welding-and-adhesive-bonding-aa6082-joints-fatigue>

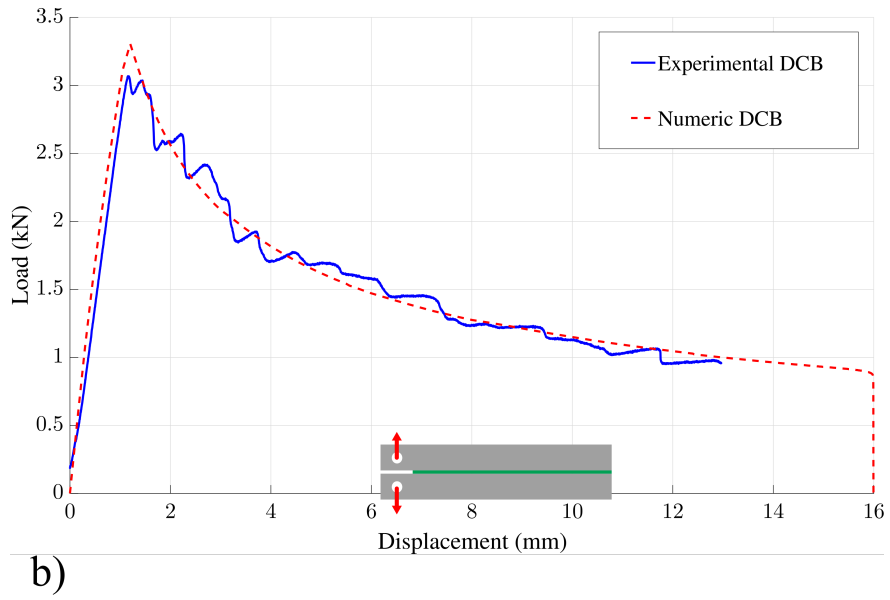
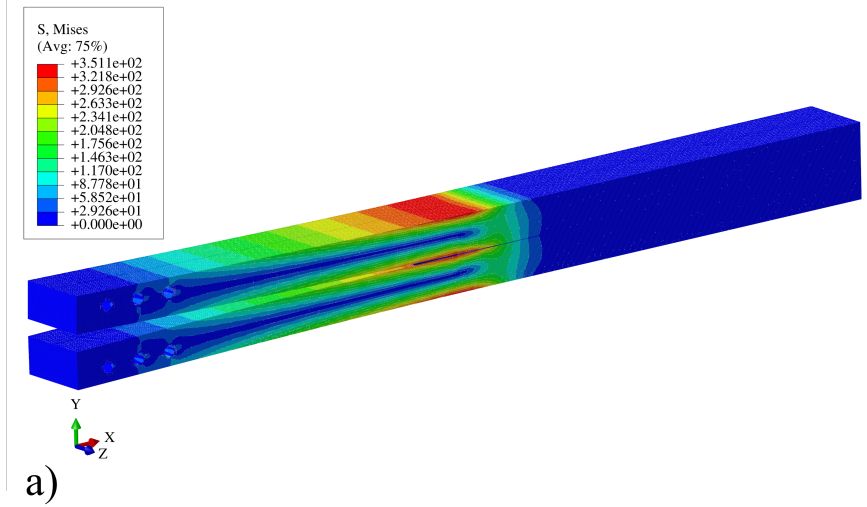
Hosted file

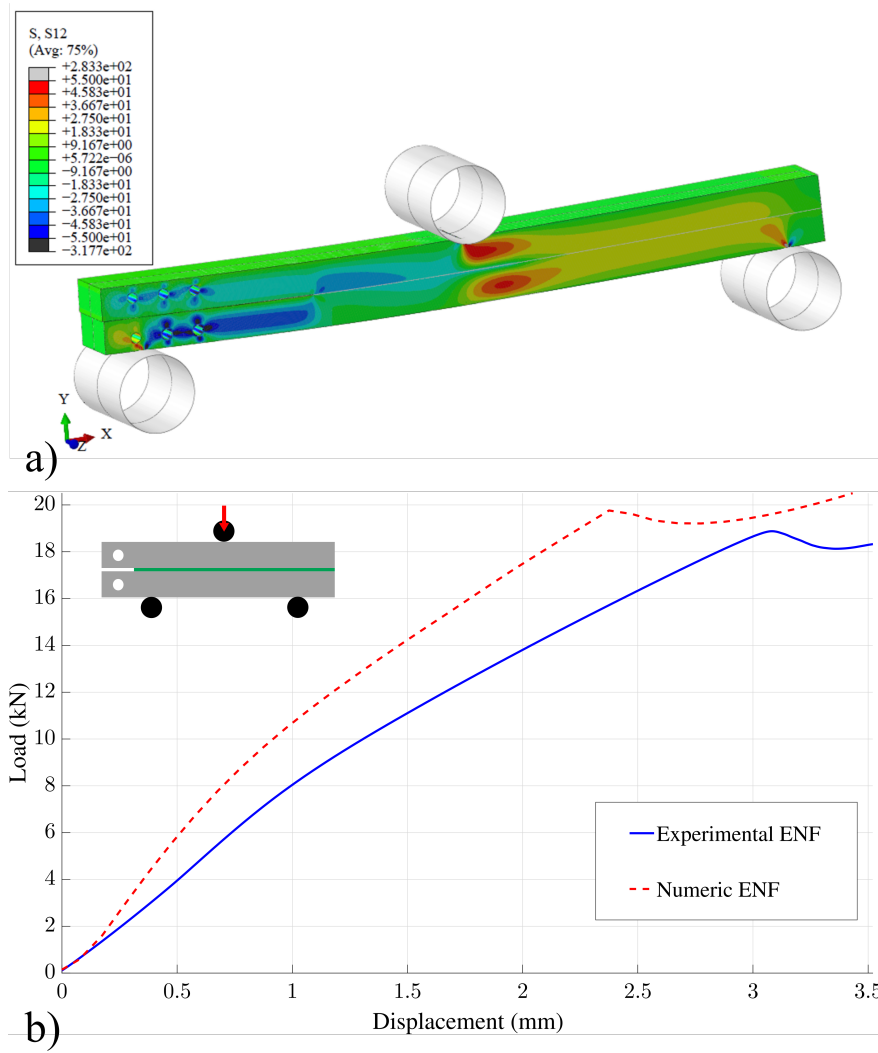
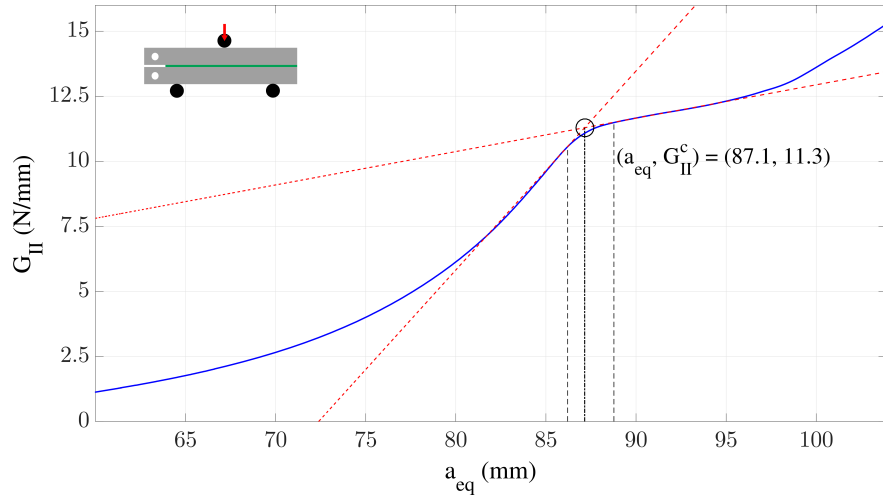
Table_4.docx available at <https://authorea.com/users/297375/articles/426489-overlap-friction-stir-welding-and-adhesive-bonding-aa6082-joints-fatigue>

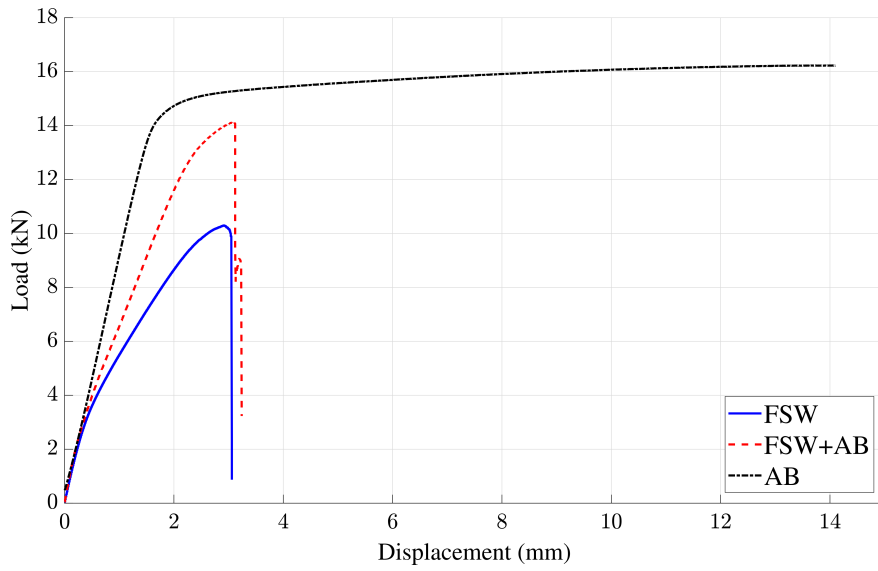
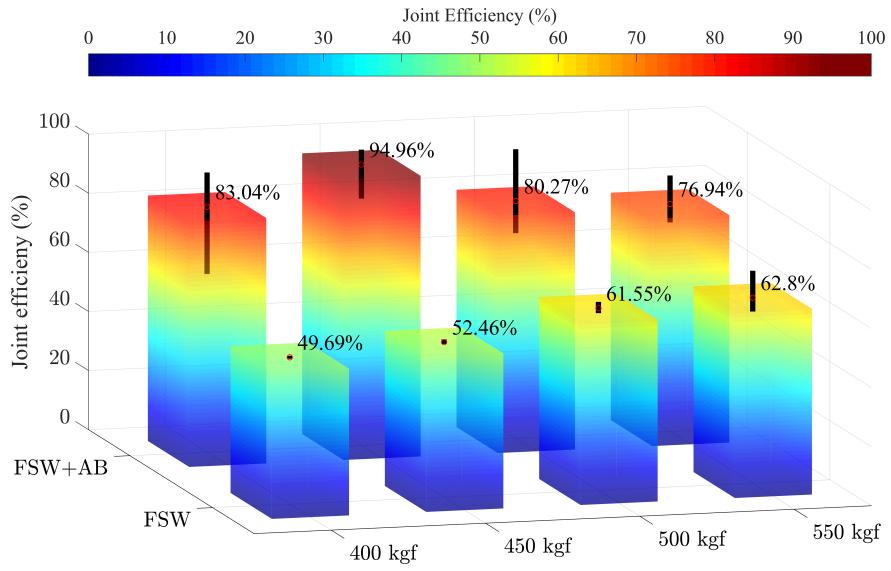


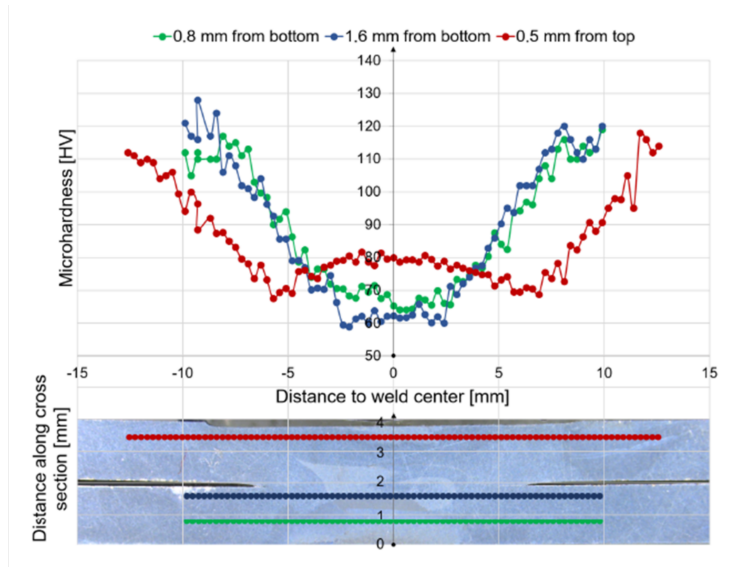




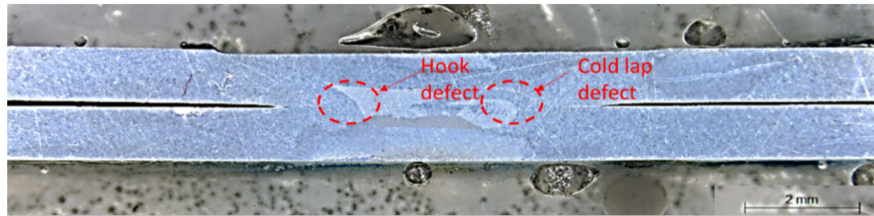




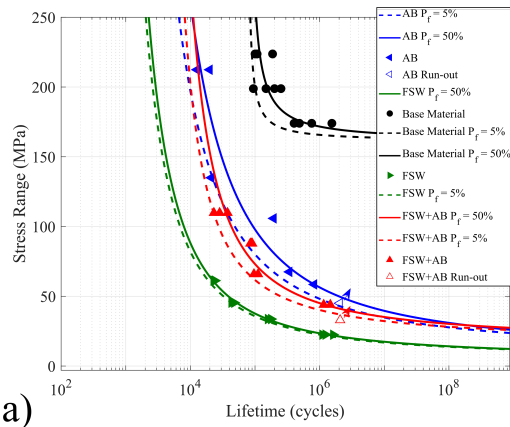




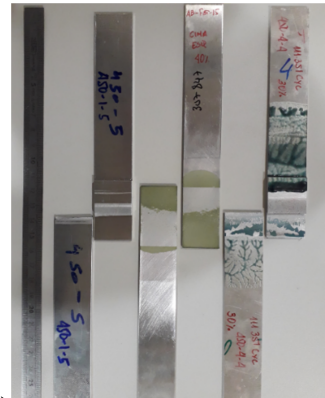
a)



b)



a)



b)